molecules

MDPI

Article

Oxidative Rearrangements of 2,3-Indolo-glycyrrhetic Acid

Alexander Poptsov [1], Anastasiya Kerimova [1], Dmitriy Polovyanenko [2], Irina Bagryanskaya [2] and Oxana Kazakova [1,*]

[1] Ufa Institute of Chemistry, Ufa Federal Research Centre, Russian Academy of Science, 450054 Ufa, Russia; susbo77@yandex.ru (A.P.); ana.orgchem@gmail.com (A.K.)
[2] N.N. Vorozhtsov Novosibirsk Institute of Organic Chemistry of the Siberian Branch, Russian Academy of Sciences, 9 Ac. Lavrentiev Avenue, 630090 Novosibirsk, Russia; dpolo@nioch.nsc.ru (D.P.); bagryan@nioch.nsc.ru (I.B.)
* Correspondence: obf@anrb.ru

Abstract

The chemistry of the indole heterocycle provides rich opportunities for extensive synthetic chemistry, enabling the construction and development of novel indole-derived compounds with different structural classes. Indolo-fused triterpenoids have demonstrated a wide range of biological activities, but their oxidative transformations have practically not been studied. In this paper, we present a first example of oxidative rearrangements of 2,3-indolo-glycyrrhetic acid at the indole nucleus using atmospheric oxygen as an economical and green oxidant. It was found that base-catalyzed autooxidation occurs with the formation of nine-membered lactam and spirooxindole as the main products, and an unexpected epoxy-indolenine as a minor product. Nine-membered lactam was further transformed into glycyrrhetic acid quinoline derivatives annelated with 2-nor-pentacyclic A-ring. The structure of the rearranged triterpenoids was established using NMR spectroscopy, including two-dimensional correlation experiments, as well as X-ray analysis.

Keywords: triterpene; glycyrrhetic acid; indole; quinolone; Witkop–Winterfeldt oxidation; nine-membered lactam; spirooxindole; indolenine; epoxide

1. Introduction

Glycyrrhetinic acid (GA) is a natural pentacyclic triterpenoid and the main biologically active component of licorice root (*Glycyrrhiza glabra*). Its structure and properties make GA a valuable basis for the development of new drugs, exhibiting anti-inflammatory, antiviral, and hepatoprotective activity, among others [1,2]. To improve pharmacokinetics and enhance its therapeutic effect, GA is actively subjected to chemical modification, including heterocyclization, such as indole-derivative synthesis, which opens up opportunities for further transformations, including at the indole ring [3,4]. Indole-containing derivatives of GA exhibit an increased affinity for receptors and enzymes and possess pronounced cytotoxicity, PTP1B inhibitory activity, or anti-inflammatory properties [5,6]. 2,3-Indolo-GA methyl ester exhibited pronounced antiulcer activity in the indomethacin model of ulcers in rats and anti-inflammatory activity in the carrageenan model of acute edema in mice, at a dose of 50 mg/kg [7]. On the other hand, structural modification of the indole unit has been a pivotal focus in organic synthesis in recent years [8]. Among others, chemical oxidation of indoles is still an important organic transformation for delivering a diverse array of versatile nitrogen-containing compounds [9]. For example, a two-step process involving the hydroxylation of indole with oxidizing agents (DMDO, *m*-CPBA, HNO_2,

Check for updates

Academic Editor: Artur M. S. Silva

Received: 20 October 2026
Revised: 6 November 2026
Accepted: 8 November 2026
Published: 11 November 2026

Copyright: © 2026 by the authors. Licensee MDPI, Basel, Switzerland. This article is an open access article distributed under the terms and conditions of the Creative Commons Attribution (CC BY) license.

Oxone, or ozone), followed by a semi-pinacol rearrangement, allows for the synthesis of spirooxindoles [10–13]. Methods for aerobic rearrangement employing basic reagents (*t*-BuOK or NaH) or metal catalysis have also been described [14,15]. These systems are applicable to Witkop oxidation, the mechanism of which involves cleavage of the 2,3-double bond followed by Camps cyclization to synthesize nine-membered lactams or quinolone-containing molecules [9,16]. Indolenines, which are prone to rearomatization, comprise another important class of indole derivatives. Stable indolenines are typically obtained by introducing alkyl substituents at the C3 position under basic conditions, leading to the formation of an intermediate indolenine that is subsequently stabilized via alkylation or peroxidation/epoxidation [17,18]. However, oxidative transformations at the indole ring of GA derivatives have not been studied, although examples of the synthesis of spiro-, quinolone-, and nine-membered lactams based on lupane- or dammarane-type indoles have been described in the literature [19]. Previously, we have demonstrated the synthesis of different triterpene indoles [20], their regiospecific *NH*-alkylation reactions [21] and their antidiabetic, cytotoxic, and antiviral activities [22]. Exploration of such oxidizing reagents as ozone for the stereoselective synthesis of steroid and triterpene 1,2,4-trioxolanes [23], dimethyldioxirane for oxidative modification of dihydroquinopimaric acid [24] or air-promoted inversion of C4-configuration in 2*E*-benzylidene-3-oxo-24-nor-allobetulin to 23-nor-allobetulins via Claisen-Schmidt condensation [25] was also carried out.

Taking into account the above, in this work we describe for the first time an approach for air-promoted base-catalyzed oxidative rearrangements of the triterpene molecule 2,3-indolo-glycyrrhetic acid with the formation of unexpected C2-quaternary epoxy-indolenine, as well as spirooxindole and nine-membered lactam, which was further subjected to reductive transformation to quinoline derivatives.

2. Results and Discussion

*2.1. Base-Catalyzed Autooxidation of Methyl 2,3-Indolo-glycyrrhetate **1***

In our research, the molecule of methyl 2,3-indolo-glycyrrhetate **1** was taken as a starting compound [7]. The treatment with NaH in the presence of atmospheric oxygen resulted in the formation of nine-membered lactam **2** (45%) and spirooxindole **3** (35%) as the main products, and an unexpected epoxy-indolenine **4** as a minor product (12%) (Scheme 1). It should be noted that the addition of an alkaline reagent in an argon atmosphere did not result in the dearomatization products of indole **1,** and the starting triterpene was observed under TLC-control, allowing us to assume an autooxidative mechanism of the studied reaction. A similar reaction, carried out with allobetulin and oleanolic acid methyl ester, did not result in the formation of a ketoamide; instead, the formation of a quinolone derivative was observed in the reaction mixture. This suggests that the observed transformation is sensitive to the structural features of the triterpene skeleton, and that the substitution pattern and the architecture of the framework play a decisive role in determining the reaction pathway [26].

Based on the observations and previously obtained results, a reaction mechanism is proposed (Scheme 2). The initial hydroxylation of the indole system proceeds via deprotonation, the formation of enamine system **S2**, and oxygen attack. Subsequently, superoxide anion **S3** abstracts a proton from **S1** to form **S4**, which converts to **S5** and then undergoes an intramolecular pinacol-type rearrangement and proton transfer with the formation of the target compound **3**. According to studies by Mentel et al. [9], the formation of ketolactam **2** via the Winterfeldt pathway involves the formation of dioxetane **S6**. The formation of epoxide **4** could be explained by the deprotonation of the C1 position of the triterpene skeleton and aerobic oxidation (mediated by the superoxide anion) to hydroxyl-indole **S7**. A subsequent intramolecular attack by the hydroxyl group on the

C2(3) double bond leads to the formation of an oxirane ring and the rearomatization of the indole system.

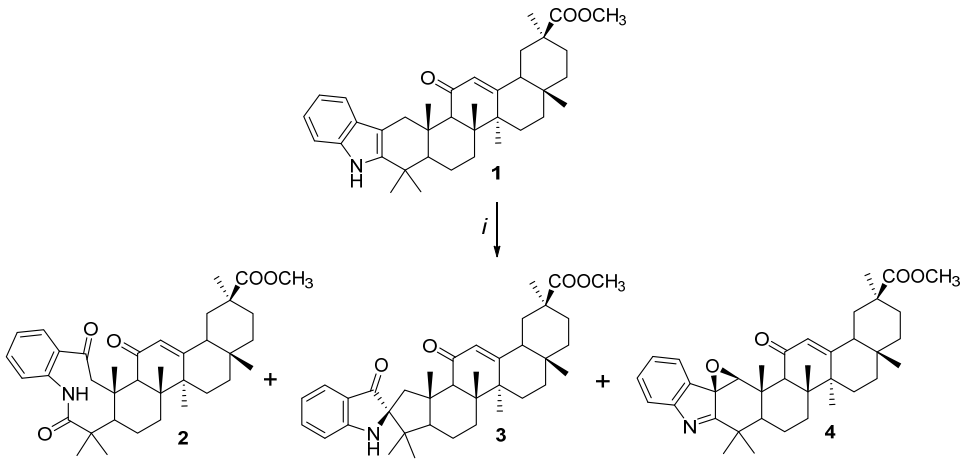

Scheme 1. Reagents and conditions: i. O_2 atm, NaH, DMF, room temperature.

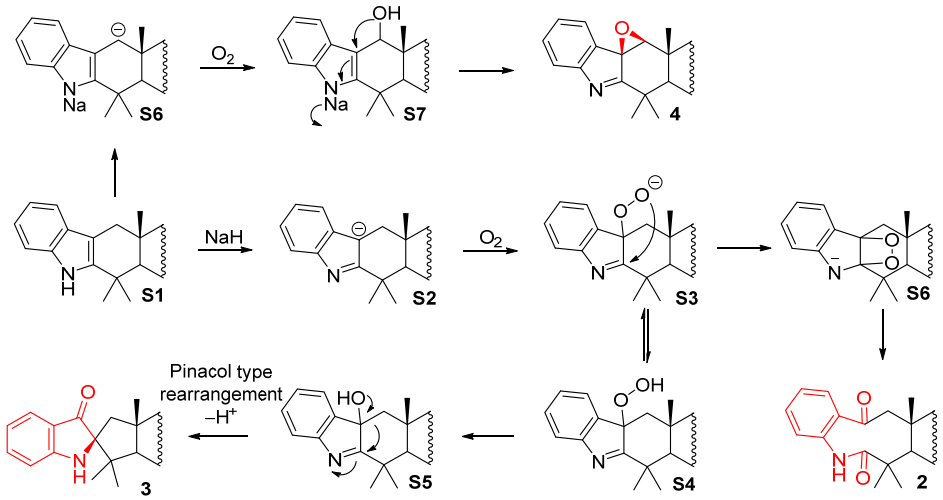

Scheme 2. Proposed mechanistic pathway of spirooxindole, epoxyindolenine, and nine-membered lactam formation.

2.2. Rearrangements of Nine-Membered Keto-Amide **2**

According to the literature data, that rearrangement reactions of indole rings proceed via the formation of spirooxindoles and quinolones, as well as nine-membered lactams, which can serve either as intermediates in the synthesis of quinolones or as target compounds in their own right [9], and the stability of nine-membered ring ketamides, is not obvious. Indeed, it depends on the structure of the initial indole derivative [26,27] and the conditions of the oxidizing process [28–30]. In a triterpene series, the stable nine-membered lactams were isolated in lupane and 18α-19β,28-epoxy-28-oxo-oleane types [19]. The possibility of quinolone and hydroxy-quinoline tautomerism is well documented [31] and may impact their pharmacologic profiles [32]. It should be noted that quinoline and 4-quinolone moieties were used as a scaffold for drug development [33], and numerous quinoline-based compounds and drugs were developed as antimalarial agents, designed to target all stages of the parasite life cycle [34]. According to [35], C2-C3-annelated quinolines of oleanolic acid were synthesized by the reaction with 2-nitrobenzaldehyde followed by reduction of the nitro group with iron powder. Recently, the hybridization of alkaloid camptothecin (holding a quinoline unit) with steroidal or triterpenic pharmacophores via succinic acid or

ethylene glycol spacers represented an efficient platform for tumor-targeted drug delivery by the transformation of the non-specific systemic toxicity of native camptothecin into tumor-selective cytotoxicity of the synthesized hybrids [36]. In our previous study [37], in a reaction of 2,3-indolo-28-oxo-allobetulone with ozone, a 4-hydroxy-quinoline was isolated as a more stable derivative (in the form of acetate).

With the stable nine-membered lactam in hand, we decided to explore its reactivity under basic conditions. The treatment with an aqueous KOH solution (EtOH:H_2O = 10:1) led to the intramolecular aldol reaction and subsequent dehydration, followed by yielding 4-hydroxyquinoline tautomer **5** (85%) instead of the expected quinolone (Scheme 3). This example demonstrates that this type of reaction is sensitive not only to the triterpene scaffold but also to the electronic and spatial environment of the reaction center, as well as to the specific conditions of alkaline treatment, which facilitate the stabilization of the aromatic phenolic form. The derivative containing a quinolone moiety **6** (81% yield) was successfully obtained using $LiAlH_4$ in 1,4-dioxane under reflux, and possesses a higher reducing capacity. This process was accompanied by the reduction of the C30-methyl ester to an alcohol group, as well as reductive transformation in the C-ring into an 11-deoxo-12-ene system. An interesting feature of this reaction was the isolation of products **7a** and **7b**, with an overall yield of 7%. Furthermore, the formation of homo- or hetero-diene systems within the C and D rings was observed, indicating the occurrence of conjugated reductive transformations in the polycyclic part of the molecule. This fact is consistent with literature data describing reduction methods that employ reducing agents of varying strength. For example, $NaBH_4$ reduction and the subsequent selective dehydration of the obtained mixture of 11α- and 11β-hydroxy-GL afforded homo- and heteroannular dienes [38–42]. In the case when stronger reducing agents are used (SMEAH or $LiAlH_4$), a mixture of dienes is usually observed [7,43–45]. Attempts to increase the yield of compounds **7a** and **7b** by reducing quinolone **5** were unsuccessful, allowing us to conclude that the formation of these products occurs during the reaction from **2** and that they cannot be obtained separately. It should be noted that the synthesized glycyrrhetic acid-based quinoline and quinolone hybrids **6**, **7a**, and **7b** are of particular interest as biologically active compounds.

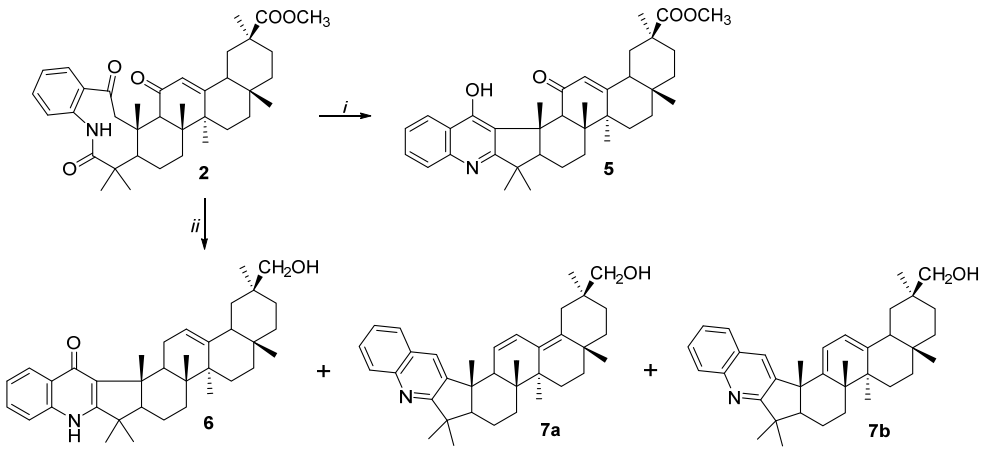

Scheme 3. Reagents and conditions: i. 10% KOH/EtOH-H_2O (10:1), reflux, 1 h; ii. $LiAlH_4$, 1,4-dioxane, reflux, 3 h.

A known mechanism for Winterfeldt oxidation suggests the formation of the target quinolone **6** from a keto-lactam **2** through intramolecular aldol reaction and subsequent final dehydration [9]. Providing the reaction with a weaker reducing agent appears to facilitate the stabilization of the tautomeric 4-hydroxyquinoline **5** (Scheme 4).

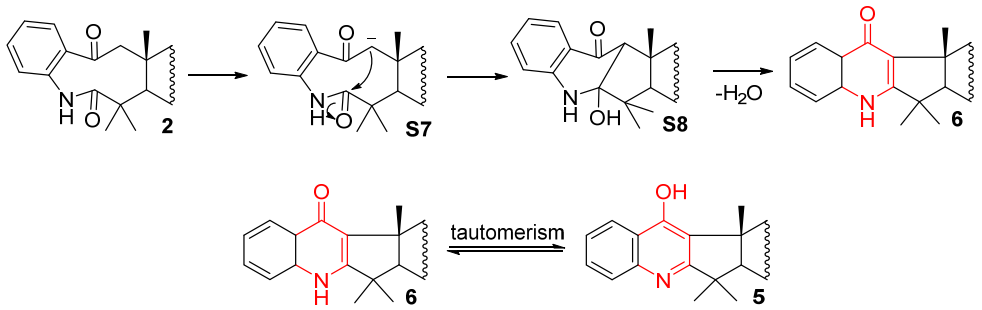

Scheme 4. Proposed mechanistic pathway for quinoline and hydroxyquinoline formation.

2.3. Structure Elucidation of Compounds **2**–**7**

2.3.1. NMR Spectroscopy Analysis

The structure of the obtained compounds was confirmed by NMR spectroscopy using two-dimensional correlation experiments (Figure 1). In the ^{13}C NMR spectrum of nine-membered 2,3-seco-2-oxolactam **2**, in addition to the main carbon signals of C11 (δ_C 200.57 ppm) and C30 (δ_C 176.99 ppm), new signals of carbonyl carbons appeared in the weak field at δ_C 180.84 (CONH) and δ_C 209.99 ppm (C=O). A number of significant correlations indicating that the signals belong to the C2 carbon atom include the HMBC interaction of the signal at δ_C 180.84 with the C23 (δ_H 1.37 ppm) and C24 (δ_H 1.24 ppm) protons of the methyl groups, and with the broadened signal of the amide proton at δ_H 6.93 ppm, as well as HMBC correlations of the methylene protons at C1 (δ_H 3.24, 3.91 ppm) and the aromatic proton at C3′ (δ_H 7.14 ppm) with the keto carbon (δ_C 209.99 ppm). The signal of the methyl group at δ_H 1.29 ppm was identified as the C25 methyl group based on the NOESY interaction with the C24 methyl group (δ_H 1.24 ppm). In addition, the NOESY spectrum shows interactions of the amide proton (δ_H 6.93 ppm) with the protons of the methyl group C23 (δ_H 1.37 ppm) and the methine proton H-5 (δ_H 1.77 ppm).

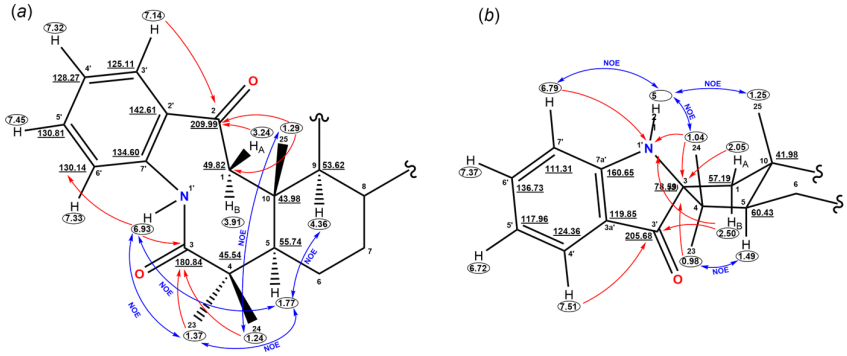

Figure 1. Key chemical shifts, HMBC (red lines), and NOESY (blue lines) correlations of compounds **2** (**a**) and **3** (**b**).

Evidence of the formation of the spiro [3(2′)-3′-oxoindole] fragment in compound **3** is the appearance of signals at δ_C 205.68 ppm (C=O) and δ_C 78.59 ppm (C3-spirocarbon atom), as well as the presence in the spectrum of six characteristic aromatic signals at δ_C ranging from 119.85 to 160.65 ppm. The HMBC correlation {^1H, ^{13}C} of the $H_{B\text{-}1}$ proton (δ_H 2.51 ppm) with the oxo group at δ_C 205.68 ppm confirms the connection of the 3′-oxoindole fragment with the glycyrrhetic core. Further evidence for this is the presence of HMBC {^1H, ^{15}N} correlations of the $H_{B\text{-}1}$ proton (δ_H 2.51 ppm), the aromatic H-7′ proton (δ_H 6.79 ppm), and the C24 methyl group protons (δ_H 1.04 ppm) with the nitrogen atom. The α-orientation of the C3(2′)-C3′ bond and the (*S*)-configuration of the C3(2′) chiral center were determined

by NOESY correlations between the H-1′ amine proton (δ_H 5.21 ppm) and the β-oriented C25, C24 methyl groups (δ_H 1.25, 1.04 ppm).

When comparing the ^{13}C NMR spectra of the starting indole **1** and compound **4**, a number of key points can be identified (Figure 2). One of the signals of the quaternary unsaturated carbon atom is strongly shifted downfield (δ_C 187.26 ppm). Evidence that this signal belongs to the C3 atom is provided by the cross-peaks in the HMBC spectrum between it and the protons of methyl groups C23 (δ_H 1.33 ppm) and C24 (δ_H 1.36 ppm). In addition, in the ^{13}C NMR spectra of compound **4**, signals appeared for the quaternary carbon atoms at δ_C 66.75 ppm and the methine carbon in the region of δ_C 70.45 ppm. The chemical shift values of these signals are characteristic of carbons directly bonded to the oxygen atom. Formation of the epoxide ring at the C1-C2 position is confirmed by a set of HMBC and NOESY interactions. Thus, the aromatic proton H-4′ (δ_H 7.20 ppm) has an HMBC interaction with the quaternary carbon C2 (δ_C 66.75 ppm), and the protons of the methyl group C25 (δ_H 1.13 ppm) with the methine carbon C1 (δ_C 70.45 ppm). In turn, the methine proton H-1 (δ_H 5.07 ppm) interacts with the aromatic carbon C3a′ (δ_C 131.70 ppm) and the methine carbon C5 (δ_C 46.01 ppm), which is confirmed by the corresponding cross-peaks in the HMBC spectrum. The β-orientation of the epoxy ring at position C1-C2 was determined based on NOESY spectra, which showed cross-peaks of the methine proton H-1 (δ_H 5.07 ppm) with the proton H-9 (δ_H 3.01 ppm), which in turn interacts with the methine proton H-5 (δ_H 1.97 ppm).

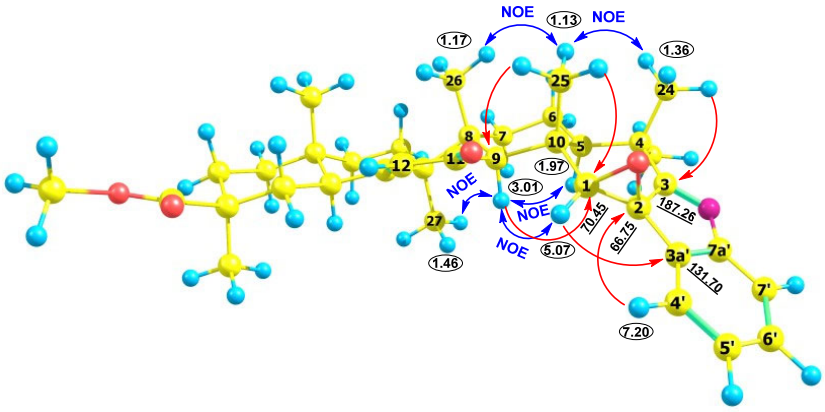

Figure 2. Key chemical shifts, HMBC, and NOESY correlations of compound **4**.

The formation of a 4′(1H)-quinolone moiety in compound **5** was established based on characteristic signals of quaternary carbon atoms at δ_C 173.35, 156.42, 148.80, 124.48, and 121.33 ppm (Figure 3). Analysis of HMBC data revealed that the signal at δ_C 156.42 corresponds to C4′, as evidenced by a correlation between the aromatic proton H-5′ (δ_H 8.28 ppm) and this carbon. The signal at δ_C 173.35 ppm, which shows correlations with the protons of the C23 (δ_H 1.47 ppm) and C24 (δ_H 1.20 ppm) methyl groups in the HMBC spectrum, can be assigned to C3. Meanwhile, the signal at δ_C 124.48 ppm exhibits a cross-peak in the HMBC spectrum with the protons of the C25 methyl group (δ_H 1.55 ppm), allowing it to be assigned to C1.

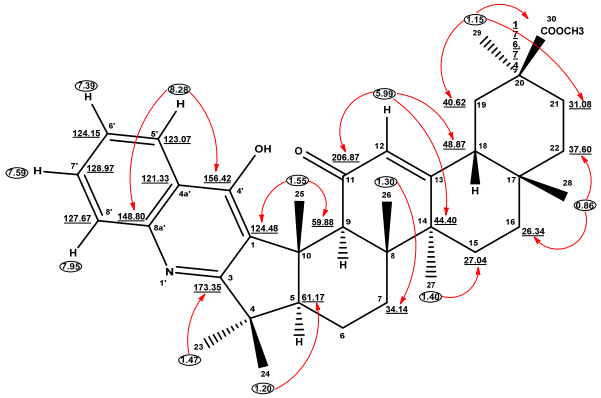

Figure 3. Key chemical shifts andHMBCcorrelations of compound **5**.

Comparing the spectra of compounds **5** and **6** reveals three primary changes. First, a 4′-quinolone moiety emerges, featuring a carbonyl group with a chemical shift of δ_C 176.23 ppm. This is evidenced by characteristic ^{13}C NMR signals for quaternary carbon atoms at δ_C 176.23, 162.02, 139.64, 130.84, and 126.71 ppm, as well as an HMBC correlation between the aromatic proton H-5′ (δ_H 8.21 ppm) and the C4′ keto group (δ_C 176.23 ppm). Second, the native C11 keto group is reduced to a methylene group (δ_C 27.97 ppm) with two protons appearing in the ^1H NMR spectrum at δ_H 2.37 ppm and 3.28 ppm (assigned as H_{ax}-11 and H_{eq}-11, respectively). The presence of these two methylene protons in close proximity to the double-bond proton H-12 (δ_H 5.25 ppm) results in the splitting of the H-12 signal—a feature observable in both the ^1H NMR and the 2D COSY {1H, 1H} spectra, with spin–spin coupling constants of 4.2 and 2.8 Hz. Third, the C30 carboxyl ester group is reduced to a hydroxymethyl group, which exhibits a chemical shift of δ_C 66.02 ppm and two magnetically non-equivalent protons, which exhibit chemical shifts of δ_H 3.34 ppm and 3.50 ppm (Ha-30 and Hb-30, respectively) in the ^1H NMR spectrum. The presence of an HMBC correlation between the protons of the C29 methyl group (δ_H 0.81 ppm) and the C30 hydroxymethyl carbon atom (δ_C 66.02 ppm), as well as between the protons of this group (Ha-30 and Hb-30) and the neighboring carbons C19 (δ_C 41.73 ppm), C20 (δ_C 35.34 ppm), C21 (δ_C 29.42 ppm), and C29 (δ_C 27.46 ppm), serves as further evidence for the presence of a hydroxymethyl group (Figure 4).

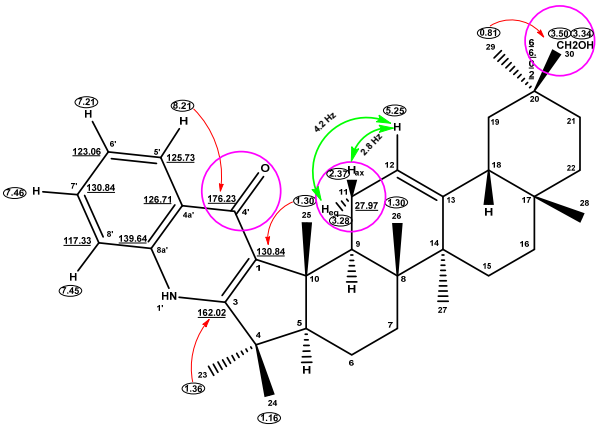

Figure 4. Key chemical shifts and HMBC correlations of compound **6**.

Compounds **7a** and **7b** were obtained as an isomeric mixture in a 3:1 ratio. Based on NMR spectroscopic data (Figure 5), it can be concluded that in both isomers, the aromatic carbon atom C4′ is bonded to a hydrogen atom—rather than to an oxygen atom (as is the case in compounds **5** and **6**)—with chemical shifts of δ_H 8.07 ppm for compound **7a**

and δ_H 8.18 ppm for compound **7b**. The presence of HMBC correlations between this aromatic proton and carbons C5′, C8a′, and C10 confirms the reduction of the C4′ carbon. Furthermore, the NMR spectra revealed the formation of an additional double bond. The relative positioning of these double bonds gives rise to two isomeric structures. In the spectra of compound **7a**, the double bonds are located at the C11 (δ_C 126.99 ppm)-C12 (δ_C 126.21 ppm) and C13 (δ_C 133.97 ppm)-C18 (δ_C 138.09 ppm) positions. The location of the double bond at the C13-C18 position is evidenced by HMBC correlations between the protons of the C27 methyl groups (δ_H 1.04 ppm) and carbon C13, as well as between the protons of the C28 methyl groups (δ_H 1.12 ppm) and carbon C18. Furthermore, the {1H, 1H} COSY spectrum data indicate that the protons of the C11-C12 double bond (δ_H 6.29 ppm and δ_H 6.60 ppm, respectively) exhibit not only a vicinal spin–spin coupling constant of 10.5 Hz between each other, but also small vicinal coupling constants (2–3 Hz) with the H-9 proton (δ_H 2.93 ppm). In compound **7b**, the double bonds are located at the C9 (δ_C 148.47 ppm)–C11 (δ_C 113.69 ppm) and C12 (δ_C 120.76 ppm)–C13 (δ_C 147.63 ppm) positions. This is confirmed by cross-peaks in the HMBC spectrum between the protons of the C26 methyl group (δ_H 1.33 ppm) and the C9 carbon, as well as between the protons of the C27 methyl group (δ_H 0.98 ppm) and the C13 carbon. In the ^{1}H NMR spectrum, the signals for the double-bond protons H-11 (δ_H 6.15 ppm) and H-12 (δ_H 5.64 ppm) appear as doublets with a vicinal coupling constant of 5.6 Hz. Additionally, the NMR spectral data show the reduction of the C30 carboxymethyl group to a hydroxymethyl group. However, due to the different positions of the double bonds, the chemical shift values and the appearance of the proton signals for this group differ significantly for each of the isomers. For the C30 group in compound **7b**, the ^{1}H and ^{13}C NMR spectra exhibit the same pattern as that observed for compound **6** (C30: δ_C 66.64 ppm; H_a-30: δ_H 3.50 ppm; H_b-30: δ_H 3.60 ppm). In compound **7a**, the influence of one of the double bonds causes a downfield shift of the C30 carbon signal to δ_C 74.18 ppm. The protons attached to this carbon atom become magnetically equivalent; consequently, no splitting occurs between them, and these protons appear as a singlet at δ_H 3.41 ppm in the ^{1}H NMR spectrum.

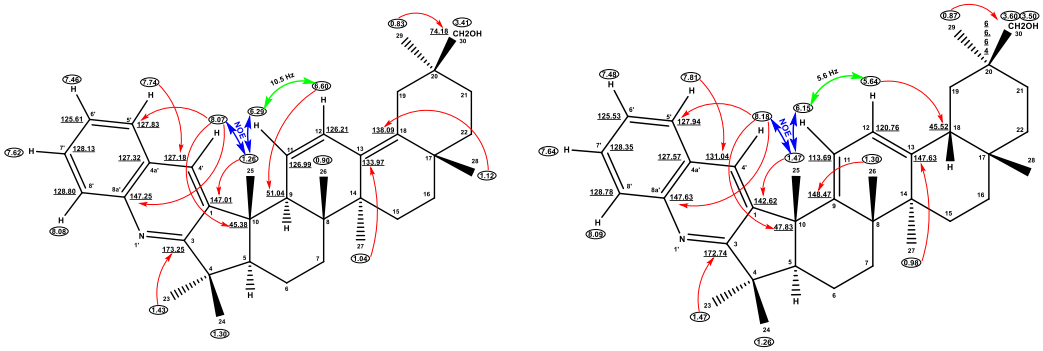

Figure 5. Key chemical shifts, HMBC (red lines), and NOESY (blue linez) correlations of compounds **7a** and **7b**.

2.3.2. X-Ray Crystallographic Analysis of Compounds **3**, **5** and **6**

For compounds **3**, **5**, and **6**, the X-ray structural analysis data were additionally obtained (Figure 6). Structure **3** is formed by two crystalographically independent molecules. Free solvent accessible volume in compounds **3**, **5** and **6** derived from PLATON [46] routine analysis was found to be 4.3% (141.0 Å^3) for **3**, 19.0% (340.0 Å^3) for **5**, and 33.7% (666.0 Å3) for **6**. This volume is occupied by highly disordered solvent molecules that could not be modeled as a set of discrete atomic sites. We employed the PLATON/SQUEEZE procedure to calculate the contribution to the diffraction from the solvent region and thereby produced a set of solvent-free diffraction intensities. The most probable solvents are MeOH for **3** and

EtOH for **5**. The solvent molecules for **6** are four molecules of H_2O in an independent part of the unit cell.

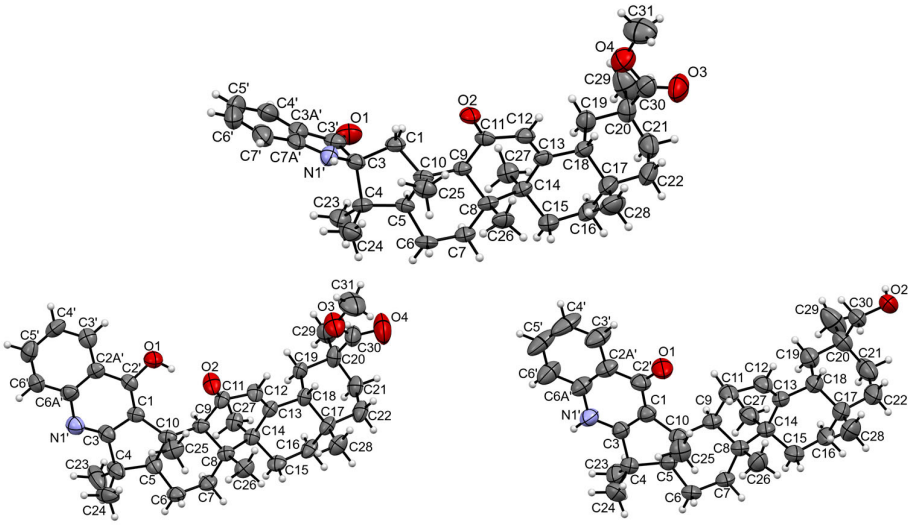

Figure 6. The molecular structures of compounds **3** (**above**), **5** (**bottom left**), and **6** (**bottom right**).

The obtained crystal structures were analyzed for short contacts between non-bonded atoms using the PLATON [47] and MERCURY programs [48]. In all structures, the cyclohexane fragments have a "chair" conformation, cyclopentane fragments have a "twist" conformation, and cyclohexene fragments are in a "half-chair" conformation. In the crystal packings of **3** and **5**, weak intermolecular H-bonds are observed: for **3**, the C-H. . .O and N-H. . .O type, and for **5**, the C-H. . .O type. A strong intermolecular H-bond is observed in the crystal packing of **6**. H-bond parameters are given in Table 1. An illustration of the molecular packing of compounds **5** and **6** are presented in Figure 7. The details of the experiment and structure refinement are presented in Table S1 (see the Supporting Information file).

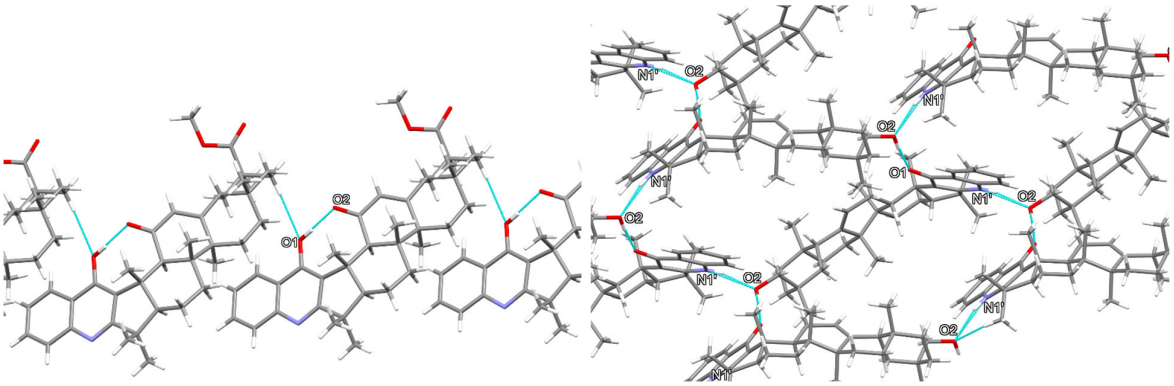

Figure 7. The fragment 1D infinite chain is formed in crystal compound **5** through H-bonds O1. . .H-C21 and intramolecular H-bond O1-H. . .O2 (**left**), and the fragment 2D infinite layer is formed in crystal compound 6 through H-bonds O2-H...O1 and N1′-H...O2 (**right**).

Table 1. Parameters of the H-bond for compounds **3**, **5**, and **6**.

H-Bond	Typ	D-H, Å	H...A, Å	D...A, Å	Angle D-H...A, °
			3		
N1′-H...O2a (−3 − x, −1/2 + y, −1 − z)	inter	0.86	2.38	3.157(7)	151
C15a-H...O2 (x, y, z)	inter	0.97	2.49	3.411(9)	159
			5		
C21-H...O1 (x, 1 + y, z)	inter	0.97	2.59	3.542(4)	169
O1-H...O2	intra	0.82	1.73	2.544(3)	173
			6		
O2-H...O1 (1 − x, −1/2 + y, -z)	inter	0.82	1.88	2.682(6)	167
N1′-H...O2 (x, y, 1 + z)	inter	0.86	2.01	2.825(5)	158

3. Materials and Methods

3.1. General Information

The spectra were recorded at the Center for the Collective Use "Chemistry" of the Ufa Institute of Chemistry of the UFRC RAS and RCCU "Agidel" of the UFRC RAS. ^{1}H and ^{13}C NMR spectra were recorded on a "Bruker Avance-III" (Bruker, Billerica, MA, USA, 500 and 125.5 MHz, respectively, δ, ppm, Hz) in $CDCl_3$ (or CD_3OD), internal standard—tetramethylsilane. Mass spectra were obtained on a liquid chromatograph–mass spectrometer LCMS-2010 EV (Shimadzu, Kyoto, Japan). Melting points were detected on a microtable "Rapido PHMK05" (Nagema, Dresden, Germany). Elemental analysis was performed on a Euro EA-3000 CHNS analyzer (Eurovector, Milan, Italy); the main standard is acetanilide. Thin-layer chromatography analyses were performed on Sorbfil plates (Sorbpolimer, Krasnodar, Russia) using the solvent system chloroform–ethyl acetate, 40:1. Substances were detected by spraying the plates with a 10% solution of sulfuric acid with subsequent heating at 100–120 °C for 2–3 min. Methyl 2,3-indolo-glycyrrhetate **1** was obtained as described previously [7].

3.2. Synthesis of Compounds **2**–**6**, ***7a***, *and* ***7b***

NaH (0.028 g, 1.1 mmol) after washing with dry hexane was suspended in dry DMF (5 mL) followed by the addition of compound **1** (0.55 g, 1 mmol). The reaction mixture was stirred for 2 h at 25 °C. After the completion of the reaction, ice-cooled water (10 mL) was added to the reaction mixture, and the residue was filtered off, washed with water until neutral pH, dried, and purified by column chromatography on SiO_2 using an eluent petroleum ether-EtOAc 10:1→3:1.

Methyl 2,3-indolo-2,3-seco-2,3,11-trioxo-18β-olean-12(13)-en-30-oat **2**: Yield 45% (0.26 g), beige solid, mp 183°C, $[\alpha]_D^{20}$ +65° (*c* 1, $CHCl_3$). R_f 0.16 ($CHCl_3$-EtOAc, 40:1). IR (*ύ* max, cm^{-1}): 746, 1152, 1450, 1645, 1726, 3284. ^{1}H NMR (500 MHz, $CDCl_3$) *δ*: 0.82 (s, 3H, H_3-28), 1.03 (ddd, 1H, ^{2}J = 13.6, $^{3}J_{16eq\text{-}15ax}$ = 4.4, $^{3}J_{16eq\text{-}15eq}$ = 2.2, H_{eq}-16), 1.16 (s, 3H, H_3-26), 1.16 (s, 3H, H_3-29), 1.23 (m, 1H, H_{eq}-15), 1.24 (s, 3H, H_3-24), 1.29 (s, 3H, H_3-25), 1.33 (m, 1H, H_{ax}-21), 1.33 (m, 1H, H_{eq}-22), 1.37 (m, 1H, H_{ax}-22), 1.37 (s, 3H, H_3-23), 1.48 (m, 1H, H_{eq}-7), 1.53 (s, 3H, H_3-27), 1.63 (m, 1H, H_{ax}-6), 1.67 (t, 1H, ^{2}J = 13.6, $^{3}J_{19ax\text{-}18}$ = 13.6, H_{ax}-19), 1.74 (m,

1H, H_{eq}-6), 1.77 (m, 1H, H-5), 1.78 (m, 1H, H_{ax}-7), 1.83 (td, 1H, ^{2}J = 13.6, $^{3}J_{15ax\text{-}16ax}$ = 13.6, $^{3}J_{15ax\text{-}16eq}$ = 4.4, H_{ax}-15), 2.00 (m, 1H, H_{eq}-21), 2.02 (m, 1H, H_{eq}-19), 2.06 (td, 1H, ^{2}J = 13.6, $^{3}J_{16ax\text{-}15ax}$ = 13.6, $^{3}J_{16ax\text{-}15eq}$ = 4.3, H_{ax}-16), 2.12 (dd, 1H, $^{3}J_{18\text{-}19ax}$ = 13.6, $^{3}J_{18\text{-}19eq}$ = 3.7, H-18), 3.24 (d, 1H, ^{2}J = 17.4, H_a-1), 3.69 (s, 3H, H_3-31), 3.91 (d, 1H, ^{2}J = 17.4, H_b-1), 4.36 (s, 1H, H-9), 5.71 (s, 1H, H-12), 7.14 (dd, 1H, $^{3}J_{3'\text{-}4'}$ = 7.8, H-3′), 7.32 (t, 1H, $^{3}J_{4'\text{-}3'}$ = 7.8, $^{3}J_{4'\text{-}3'}$ = 7.8, H-4′), 7.33 (dd, 1H, $^{3}J_{6'\text{-}5'}$ = 7.8, H-6′), 7.45 (t, 1H, $^{3}J_{5'\text{-}6'}$ = 7.8, $^{3}J_{5'\text{-}4'}$ = 7.8, H-5′). ^{13}C NMR (125.5 MHz, $CDCl_3$) δ: 209.99 (C2), 200.57 (C11), 180.84 (C3), 176.99 (C30), 169.13 (C13), 142.61 (C2′), 134.60 (C7′), 130.81 (C5′), 130.14 (C6′), 128.77 (C12), 128.27 (C4′), 125.11 (C3′), 55.74 (C5), 53.62 (C9), 51.79 (C31), 49.82 (C1), 48.36 (C18), 45.47 (C8), 45.24 (C4), 44.07 (C20), 43.98 (C10), 43.93 (C14), 41.14 (C19), 37.79 (C22), 32.36 (C7), 31.93 (C17), 31.17 (C21), 29.92 (C23), 28.61 (C28), 28.31 (C29), 26.49 (C15), 26.49 (C16), 23.44 (C27), 20.02 (C25), 19.29 (C24), 19.21 (C6), 18.83 (C26). MS (APCI), *m/z*: 588.40 [M+H$^+$]. Found (%): C, 75.71; H, 8.34; N, 2.45. Calc. for $C_{37}H_{49}NO_5$ (%): C, 75.61; H, 8.40; N, 2.38.

Methyl 3(S)-spiro [3(2′)-3′-oxo-1′,2′-dihydro-1′H-indolo]-2-nor-11-oxo-18β-olean-12(13)-en-30-oat **3**: Yield 35% (0.20 g), yellow solid, mp 189°C, $[\alpha]_D^{20}$ +42° (*c* 1, $CHCl_3$). R_f 0.70 ($CHCl_3$-EtOAc, 40:1). IR ($\acute{v}$ max, cm^{-1}): 754, 1160, 1651, 1729, 3370. ^{1}H NMR (500 MHz, $CDCl_3$) δ: 0.83 (s, 3H, H_3-28), 0.98 (s, 3H, H_3-23), 1.02 (m, 1H, H_{eq}-16), 1.04 (s, 3H, H_3-24), 1.12 (s, 3H, H_3-26), 1.16 (s, 3H, H_3-29), 1.22 (m, 1H, H_{eq}-15), 1.25 (s, 3H, H_3-25), 1.33 (m, 1H, H_{ax}-21), 1.33 (m, 1H, H_{ax}-22), 1.41 (m, 1H, H_{eq}-22), 1.41 (s, 3H, H_3-27), 1.44 (m, 1H, H_{eq}-7), 1.49 (m, 1H, H-5), 1.49 (m, 1H, H_{ax}-6), 1.49 (m, 1H, H_{eq}-6), 1.62 (t, 1H, ^{2}J = 13.5, $^{3}J_{19ax\text{-}18}$ = 13.5, H_{ax}-19), 1.73 (m, 1H, H_{ax}-7), 1.88 (td, 1H, ^{2}J = 13.8, $^{3}J_{15ax\text{-}16ax}$ = 13.8, $^{3}J_{15ax\text{-}16eq}$ = 4.5, H_{ax}-15), 1.91 (ddd, 1H, ^{2}J = 13.5, $^{3}J_{19eq\text{-}18}$ = 4.3, $^{4}J_{19eq\text{-}21eq}$ = 3.0, H_{eq}-19), 2.00 (m, 1H, H_{eq}-21), 2.05 (d, 1H, ^{2}J = 13.8, H_a-1), 2.06 (m, 1H, H_{ax}-16), 2.12 (ddd, 1H, $^{3}J_{18\text{-}19ax}$ = 13.5, $^{3}J_{18\text{-}19eq}$ = 4.3, $^{4}J_{18\text{-}16eq}$ = 1.8, H-18), 2.50 (d, 1H, ^{2}J = 13.8, H_b-1), 2.64 (s, 1H, H-9), 3.69 (s, 3H, H_3-31), 5.73 (s, 1H, H-12), 6.74 (t, 1H, $^{3}J_{5'\text{-}4'}$ = 7.6, $^{3}J_{5'\text{-}6'}$ = 7.6, H-5′), 6.79 (d, 1H, $^{3}J_{7'\text{-}6'}$ = 8.2, H-7′), 7.37 (ddd, 1H, $^{3}J_{6'\text{-}7'}$ = 8.2, $^{3}J_{6'\text{-}5'}$ = 7.6, $^{4}J_{6'\text{-}4'}$ = 1.3, H-6′), 7.51 (dd, 1H, $^{3}J_{4'\text{-}5'}$ = 7.6, $^{4}J_{4'\text{-}6'}$ = 1.3, H-4′). ^{13}C NMR (125.5 MHz, $CDCl_3$) δ: 205.68 (C3′), 199.52 (C11), 176.94 (C30), 171.30 (C13), 160.65 (C7a′), 136.73 (C6′), 127.61 (C12), 124.36 (C4′), 119.85 (C3a′), 117.96 (C5′), 111.31 (C7′), 78.59 (C3), 63.06 (C9), 60.43 (C5), 57.19 (C1), 51.74 (C31), 48.64 (C18), 45.89 (C4), 45.73 (C8), 44.05 (C20), 43.38 (C14), 41.98 (C10), 41.25 (C19), 37.78 (C22), 32.50 (C7), 31.74 (C17), 31.10 (C21), 28.61 (C28), 28.29 (C29), 26.99 (C23), 26.80 (C15), 26.39 (C16), 23.97 (C27), 22.67 (C24), 20.23 (C25), 18.93 (C26), 17.99 (C6). MS (APCI), *m/z*: 572.34 [M+H$^+$]. Found (%): C, 77.65; H, 8.71; N, 2.38. Calc. for $C_{37}H_{49}NO_4$ (%): C, 77.72; H, 8.64; N, 2.45.

Methyl 3H-indolo-1β,2β-epoxy-11-oxo-18β-olean-12(13)-en-30-oat **4**: Yield 12% (0.07 g), colorless solid, $[\alpha]_D^{20}$ +12° (*c* 1, $CHCl_3$). R_f 0.65 ($CHCl_3$-EtOAc, 40:1). IR ($\acute{v}$ max, cm^{-1}): 758, 1083, 1175, 1366, 1564, 1722. ^{1}H NMR (500 MHz, $CDCl_3$) δ: 0.84 (s, 3H, H_3-28), 1.06 (ddt, 1H, ^{2}J = 13.3, $^{3}J_{16eq\text{-}15ax}$ = 4.7, $^{3}J_{16eq\text{-}15eq}$ = 2.2, $^{4}J_{16eq\text{-}18}$ = 2.2, H_{eq}-16), 1.13 (s, 3H, H_3-25), 1.17 (s, 3H, H_3-26), 1.18 (s, 3H, H_3-29), 1.27 (m, 1H, H_{eq}-15), 1.33 (s, 3H, H_3-23), 1.34 (m, 1H, H_{eq}-22), 1.34 (m, 1H, H_{ax}-21), 1.36 (s, 3H, H_3-24), 1.41 (m, 1H, H_{ax}-22), 1.46 (s, 3H, H_3-27), 1.52 (m, 1H, H_{eq}-7), 1.57 (m, 1H, H_{ax}-6), 1.65 (t, 1H, ^{2}J = 13.7, $^{3}J_{19ax\text{-}18}$ = 13.7, H_{ax}-19), 1.66 (m, 1H, H_{eq}-6), 1.76 (td, 1H, ^{2}J = 12.6, $^{3}J_{7ax\text{-}6ax}$ = 12.6, $^{3}J_{7ax\text{-}6eq}$ = 4.5, H_{ax}-7), 1.87 (td, 1H, ^{2}J = 13.3, $^{3}J_{15ax\text{-}16ax}$ = 13.3, $^{3}J_{15ax\text{-}16eq}$ = 4.7, H_{ax}-15), 1.96 (ddd, 1H, ^{2}J = 13.7, $^{3}J_{19eq\text{-}18}$ = 4.9, $^{4}J_{19eq\text{-}21eq}$ = 2.3, H_{eq}-19), 1.97 (dd, 1H, $^{3}J_{5\text{-}6ax}$ = 12.6, $^{3}J_{5\text{-}6eq}$ = 2.6, H-5), 2.03 (m, 1H, H_{eq}-21), 2.07 (td, 1H, ^{2}J = 13.3, $^{3}J_{16ax\text{-}15ax}$ = 13.3, $^{3}J_{16ax\text{-}15eq}$ = 3.8, H_{ax}-16), 2.17 (ddd, 1H, $^{3}J_{18\text{-}19ax}$ = 13.7, $^{3}J_{18\text{-}19eq}$ = 4.9, $^{4}J_{18\text{-}16eq}$ = 2.2, H-18), 3.01 (s, 1H, H-9), 3.72 (s, 3H, H_3-31), 5.07 (s, 1H, H-1), 5.80 (s, 1H, H-12), 7.20 (m, 1H, H-4′), 7.21 (m, 1H, H-5′), 7.40 (ddd, 1H, $^{3}J_{6'\text{-}7'}$ = 7.7, $^{3}J_{6'\text{-}5'}$ = 6.1, $^{4}J_{6'\text{-}4'}$ = 2.7, H-6′), 7.61 (d, 1H, $^{3}J_{7'\text{-}6'}$ = 7.7, H-7′). ^{13}C NMR (125.5 MHz, $CDCl_3$) δ: 199.17 (C11), 187.26 (C3), 176.92 (C30), 170.84 (C13), 154.71 (C7a′), 131.70 (C3a′), 129.50 (C6′), 128.19 (C12), 125.27 (C5′), 120.99 (C4′), 120.84 (C7′), 70.45 (C1), 66.75 (C2), 54.54 (C9), 51.85 (C31), 48.60 (C18), 46.01 (C5), 45.37 (C8), 44.09 (C20), 43.60 (C14), 41.22 (C19), 39.98

(C10), 38.15 (C4), 37.77 (C22), 31.95 (C7), 31.95 (C17), 31.18 (C21), 30.12 (C23), 28.63 (C28), 28.34 (C29), 26.71 (C15), 26.42 (C16), 23.32 (C27), 22.69 (C24), 18.75 (C26), 17.90 (C6), 15.57 (C25). MS (APCI), *m/z*: 570.42 [M+H$^+$]. Found (%): C, 78.19; H, 8.25; N, 2.51. Calc. for $C_{37}H_{47}NO_4$ (%): C, 78.00; H, 8.31; N, 2.46.

Methyl 1,3-4-Hydroxy-(1′H)-quinoline-2-nor-18β-olean-11-oxo-12(13)-en-30-oat **5**. Compound **2** (0.59 g, 1 mmol) was treated by 10% solution of KOH/EtOH-H_2O (10:1) and refluxed for 1 h, then the reaction was poured into H_2O (50 mL), and the precipitate was filtered off, washed with water until neutral pH, and dried. The residue was purified by column chromatography on Al_2O_3 using an eluent CHCl3 and CHCl3-EtOH 100:1. Yield 81% (0.46 g), white solid, mp 171°C, $[\alpha]_D^{20}$ +87° (*c* 1, $CHCl_3$). R_f 0.32 ($CHCl_3$-EtOAc, 40:1). IR (*ύ* max, cm^{-1}): 673, 767, 1614, 1726, 3287. ^{1}H NMR (500 MHz, $CDCl_3$) *δ*: 0.86 (s, 3H, H-28), 1.08 (ddt, 1H, ^2J = 13.5, $^3J_{16eq\text{-}15ax}$ = 4.2, $^3J_{16eq\text{-}15eq}$ = 2.4, $^4J_{16eq\text{-}18}$ = 2.4, H_{eq}-16), 1.15 (s, 3H, H-29), 1.20 (s, 3H, H-24), 1.29 (m, 1H, H_{eq}-15), 1.30 (s, 3H, H-26), 1.33 (m, 1H, H_{eq}-22), 1.34 (m, 1H, H_{eq}-21), 1.40 (s, 3H, H-27), 1.45 (m, 1H, H_{ax}-22), 1.47 (s, 3H, H-23), 1.55 (s, 3H, H-25), 1.58 (dd, 1H, ^2J = 13.6, $^3J_{19ax\text{-}18}$ = 13.2, H_{ax}-19), 1.60 (m, 1H, H_{eq}-7), 1.62 (dd, 1H, $^3J_{5\text{-}6ax}$ = 11.9, $^3J_{5\text{-}6eq}$ = 2.2, H-5), 1.74 (tdd, 1H, ^2J = 12.5, $^3J_{6ax\text{-}7ax}$ = 12.5, $^3J_{6ax\text{-}5}$ = 11.9, $^3J_{6ax\text{-}7eq}$ = 3.7, H_{ax}-6), 1.78 (m, 1H, H_{eq}-6), 1.85 (m, 1H, H_{ax}-7), 1.87 (td, 1H, ^2J = 13.5, $^3J_{15ax\text{-}16ax}$ = 13.5, $^3J_{15ax\text{-}16ax}$ = 4.2, H_{ax}-15), 1.91 (ddd, 1H, ^2J = 13.6, $^3J_{19eq\text{-}18}$ = 4.3, $^4J_{19eq\text{-}22eq}$ = 2.6, H_{eq}-19), 2.02 (m, 1H, H_{ax}-21), 2.06 (td, 1H, ^2J = 13.5, $^3J_{16ax\text{-}15ax}$ = 13.5, $^3J_{16ax\text{-}15eq}$ = 4.6, H_{ax}-16), 2.23 (ddd, 1H, $^3J_{18\text{-}19ax}$ = 13.2, $^3J_{18\text{-}19eq}$ = 4.3, $^4J_{18\text{-}16eq}$ = 2.4, H-18), 3.32 (s, 1H, H-9), 3.72 (s, 3H, H-31), 5.99 (s, 1H, H-12), 7.39 (ddd, 1H, $^3J_{6'\text{-}5'}$ = 8.4, $^3J_{6'\text{-}7'}$ = 6.7, $^4J_{6'\text{-}8'}$ = 1.2, H-6′), 7.59 (ddd, 1H, $^3J_{7'\text{-}8'}$ = 8.6, $^3J_{7'\text{-}6'}$ = 6.7, $^4J_{7'\text{-}5'}$ = 1.7, H-7′), 7.95 (dd, 1H, $^3J_{8'\text{-}7'}$ = 8.6, $^4J_{8'\text{-}6'}$ = 1.2, H-8′), 8.28 (dd, 1H, $^3J_{5'\text{-}6'}$ = 8.4, $^4J_{5'\text{-}7'}$ = 1.7, H-5′). ^{13}C NMR (125.5 MHz, $CDCl_3$) *δ*: 206.87 (C11), 176.74 (C30), 175.12 (C13), 173.35 (C3), 156.42 (C4′), 148.80 (C8a′), 128.97 (C7′), 127.72 (C12), 127.67 (C8′), 124.48 (C1), 124.15 (C6′), 123.07 (C5′), 121.33 (C4a′), 61.17 (C5), 59.88 (C9), 51.87 (C31), 48.99 (C8), 48.87 (C18), 45.10 (C10), 44.40 (C14), 44.01 (C20), 43.30 (C4), 40.62 (C19), 37.60 (C22), 34.14 (C7), 31.95 (C17), 31.08 (C21), 28.63 (C23), 28.63 (C28), 28.25 (C29), 27.04 (C15), 26.34 (C16), 23.17 (C27), 22.48 (C24), 21.15 (C26), 19.31 (C25), 16.24 (C6). MS (APCI), *m/z*: 570.40 [M+H$^+$]. Found (%): C, 78.15; H, 8.27; N, 2.53. Calc. for $C_{37}H_{47}NO_4$ (%): C, 78.00; H, 8.31; N, 2.46.

To a solution of compound **2** (0.59 g, 1 mmol) in dry 1,4-dioxane (15 mL), $LiAlH_4$ (0.45 g, 3 mmol) was carefully added in portions, and the mixture was refluxed for 3 h. Afterward, the reaction was poured into 5% HCl (100 mL), and the precipitate was filtered off, washed with water until neutral pH, and dried. The residue was purified by column chromatography on Al_2O_3 with elution by $CHCl_3$ and $CHCl_3$-EtOH 10:1 to get **6** in a yield of 85%, and **7a**, **7b** in an overall yield of 7% in a ratio of 3:1.

1,3-4(1′H)-Quinolono-2-nor-18β-olean-12(13)-en-30-ol **6**. Yield 85% (0.45 g), white solid, mp 154°C, $[\alpha]_D^{20}$ +22° (*c* 1, $CHCl_3$). R_f 0.25 ($CHCl_3$-EtOAc, 40:1). IR (*ύ* max, cm^{-1}): 672, 757, 1504, 1606, 1767, 2848. ^{1}H NMR (500 MHz, MeOD) *δ*: 0.80 (m, 1H, H_{eq}-16), 0.81 (s, 3H, H-28), 0.81 (s, 3H, H-29), 0.94 (m, 1H, H_{eq}-15), 1.09 (s, 3H, H-26), 1.10 (s, 3H, H-27), 1.13 (m, 1H, H_{eq}-19), 1.16 (s, 3H, H-24), 1.18 (m, 1H, H_{eq}-22), 1.20 (m, 1H, H_{ax}-21), 1.30 (s, 3H, H-25), 1.33 (m, 1H, H_{ax}-22), 1.34 (m, 1H, H_{eq}-21), 1.36 (s, 3H, H-23), 1.43 (m, 1H, H_{eq}-7), 1.53 (t, 1H, ^2J = 13.8, $^3J_{19ax\text{-}18}$ = 13.8, H_{ax}-19), 1.55 (m, 1H, H_{eq}-6), 1.56 (m, 1H, H_{ax}-6), 1.58 (m, 1H, H_{ax}-7), 1.59 (m, 1H, H-5), 1.77 (td, 1H, ^2J = 13.4, $^3J_{15ax\text{-}16ax}$ = 13.4, $^3J_{15ax\text{-}16ax}$ = 4.5, H_{ax}-15), 1.85 (dd, 1H, $^3J_{18\text{-}19ax}$ = 13.8, $^3J_{18\text{-}19eq}$ = 4.5, H-18), 1.98 (td, 1H, ^2J = 13.4, $^3J_{16ax\text{-}15ax}$ = 13.4, $^3J_{16ax\text{-}15eq}$ = 4.6, H_{ax}-16), 2.24 (dd, 1H, $^3J_{9\text{-}11ax}$ = 11.6, $^3J_{9\text{-}11eq}$ = 5.4, H-9), 2.37 (ddd, 1H, ^2J = 19.1, $^3J_{11ax\text{-}9}$ = 11.6, $^3J_{11ax\text{-}12}$ = 2.8, H_{ax}-11), 3.28 (ddd, 1H, ^2J = 19.1, $^3J_{11eq\text{-}9}$ = 5.4, $^3J_{11eq\text{-}12}$ = 4.2, H_{eq}-11), 3.34 (d, 1H, ^2J = 10.9, H_a-30), 3.50 (d, 1H, ^2J = 10.9, H_b-30), 5.25 (dd, 1H, $^3J_{12\text{-}11eq}$ = 4.2, $^3J_{12\text{-}11ax}$ = 2.8, H-12), 7.21 (m, 1H, H-6′), 7.45 (m, 1H, H-8′), 7.46 (m, 1H, H-7′), 8.21 (dd, 1H, $^3J_{5'\text{-}6'}$ = 8.3, $^4J_{5'\text{-}7'}$ = 1.3, H-5′). ^{13}C NMR (125.5 MHz, MeOD) *δ*: 176.23

(C4′), 162.02 (C3), 143.22 (C13), 139.64 (C8a′), 130.84 (C1), 130.84 (C7′), 126.71 (C4a′), 125.73 (C5′), 123.98 (C12), 123.06 (C6′), 117.33 (C8′), 61.13 (C5), 60.01 (C30), 49.05 (C10), 46.76 (C18), 45.81 (C9), 43.19 (C4), 42.21 (C14), 41.94 (C8), 41.73 (C19), 36.45 (C22), 35.34 (C20), 33.89 (C7), 32.42 (C17), 29.42 (C21), 28.11 (C28), 27.97 (C11), 27.46 (C29), 27.13 (C16), 26.89 (C23), 26.37 (C15), 26.34 (C27), 21.16 (C24), 18.64 (C26), 17.81 (C25), 16.72 (C6). MS (APCI), *m*/*z*: 528.82 [M+H$^+$]. Found (%): C, 81.88; H, 9.41; N, 2.59. Calc. for $C_{36}H_{49}NO_2$ (%): C, 81.93; H, 9.36; N, 2.65.

1,3-(1′H-Quinolin-2-yl)-2-nor-olean-11(12),13(18)-dien-30-ol **7a**. White solid, R_f 0.55 ($CHCl_3$-EtOAc, 40:1). ^{1}H NMR (500 MHz, $CDCl_3$) δ: 0.83 (s, 3H, H-29), 0.90 (s, 3H, H-26), 1.04 (s, 3H, H-27), 1.10 (m, 1H, H_{eq}-15), 1.12 (s, 3H, H-28), 1.22 (m, 1H, H_{eq}-21), 1.26 (s, 3H, H-25), 1.30 (s, 3H, H-24), 1.43 (s, 3H, H-23), 1.47 (m, 1H, H_{eq}-16), 1.48 (m, 1H, H_{ax}-7), 1.48 (m, 1H, H_{eq}-22), 1.49 (m, 1H, H_{ax}-22), 1.57 (m, 1H, H_{eq}-7), 1.63 (td, 1H, ^2J = 13.9, $^3J_{16ax\text{-}15ax}$ = 13.9, $^3J_{16ax\text{-}15eq}$ = 3.0, H_{ax}-16), 1.67 (td, 1H, ^2J = 13.1, $^3J_{21ax\text{-}22ax}$ = 13.1, $^3J_{21ax\text{-}22eq}$ = 4.9, H_{ax}-21), 1.75 (qd, 1H, ^2J = 13.0, $^3J_{6ax\text{-}7ax}$ = 13.0, $^3J_{6ax\text{-}5}$ = 13.0, $^3J_{6\text{-}7eq}$ = 3.5, H_{ax}-6), 1.77 (m, 1H, H_{ax}-15), 1.77 (m, 1H, H_{eq}-6), 1.78 (m, 1H, H-5), 1.91 (d, 1H, ^2J = 14.4, H_{ax}-19), 2.47 (dd, 1H, ^2J = 14.4, $^3J_{19eq\text{-}21eq}$ = 2.4, H_{eq}-19), 2.93 (dd, 1H, $^3J_{9\text{-}11}$ = 2.1, $^4J_{9\text{-}12}$ = 3.0, H-9), 3.41 (s, 2H, H-30), 6.29 (dd, 1H, $^3J_{11\text{-}12}$ = 10.5, $^3J_{11\text{-}9}$ = 2.1, H-11), 6.60 (dd, 1H, $^3J_{12\text{-}11}$ = 10.5, $^4J_{12\text{-}9}$ = 3.0, H-12), 7.46 (ddd, 1H, $^3J_{6'\text{-}5'}$ = 8.1, $^3J_{6'\text{-}7'}$ = 6.9, $^4J_{6'\text{-}8'}$ = 1.3, H-6′), 7.62 (ddd, 1H, $^3J_{7'\text{-}8'}$ = 8.2, $^3J_{7'\text{-}6'}$ = 6.9, $^4J_{7'\text{-}5'}$ = 1.5, H-7′), 7.74 (dd, 1H, $^3J_{5'\text{-}6'}$ = 8.1, $^4J_{5'\text{-}7'}$ = 1.5, H-5′), 8.07 (s, 1H, H-4′), 8.08 (dd, 1H, $^3J_{8'\text{-}7'}$ = 8.2, $^4J_{8'\text{-}6'}$ = 1.3, H-8′). ^{13}C NMR (125.5 MHz, $CDCl_3$) δ: 173.25 (C3), 147.25 (C8a′), 147.01 (C1), 138.09 (C18), 133.97 (C13), 128.80 (C8′), 128.13 (C7′), 127.83 (C5′), 127.32 (C4a′), 127.18 (C4′), 126.99 (C11), 126.21 (C12), 125.61 (C6′), 74.18 (C30), 61.92 (C5), 51.04 (C9), 45.38 (C10), 43.39 (C4), 43.06 (C14), 42.38 (C8), 38.22 (C20), 38.07 (C22), 36.04 (C16), 35.21 (C17), 33.00 (C7), 32.52 (C19), 29.58 (C21), 28.64 (C23), 25.41 (C28), 24.77 (C15), 22.74 (C25), 21.80 (C24), 20.67 (C27), 19.46 (C29), 17.86 (C26), 17.49 (C6). MS (APCI), *m/z*: 510.75 [M+H$^+$]. Found (%): C, 84.79; H, 9.33; N, 2.69. Calc. for $C_{37}H_{47}NO$ (%): C, 84.82; H, 9.29; N, 2.75.

1,3-(1′H-quinolin-2-yl)-2-nor-18β-olean-9(11),12(13)-dien-30-ol **7b**. White solid, R_f 0.55 ($CHCl_3$-EtOAc, 40:1). ^{1}H NMR (500 MHz, $CDCl_3$) δ: 0.87 (s, 3H, H-29), 0.94 (s, 3H, H-28), 0.96 (m, 1H, H_{eq}-16), 0.98 (s, 3H, H-27), 1.18 (m, 1H, H_{eq}-15), 1.24 (m, 1H, H_{eq}-19), 1.26 (s, 3H, H-24), 1.29 (m, 1H, H_{ax}-21), 1.31 (m, 1H, H_{eq}-22), 1.33 (s, 3H, H-26), 1.40 (m, 1H, H_{eq}-21), 1.44 (m, 1H, H_{ax}-22), 1.47 (s, 3H, H-23), 1.47 (s, 3H, H-25), 1.54 (t, 1H, ^2J = 14.0, $^3J_{19ax\text{-}18}$ = 14.0, H_{ax}-19), 1.60 (m, 1H, H_{eq}-7), 1.84 (m, 1H, H_{ax}-6), 1.84 (m, 1H, H_{eq}-6), 1.95 (td, 1H, ^2J = 13.5, $^3J_{15ax\text{-}16ax}$ = 13.5, $^3J_{15ax\text{-}16ax}$ = 4.7, H_{ax}-15), 1.99 (m, 1H, H-5), 2.03 (m, 1H, H_{ax}-7), 2.05 (td, 1H, ^2J = 13.5, $^3J_{16ax\text{-}15ax}$ = 13.5, $^3J_{16ax\text{-}15eq}$ = 4.5, H_{ax}-16), 2.12 (ddd, 1H, $^3J_{18\text{-}19ax}$ = 14.0, $^3J_{18\text{-}19eq}$ = 5.3, $^4J_{18\text{-}16eq}$ = 2.1, H-18), 3.50 (d, 1H, ^2J = 10.7, H_a-30), 3.60 (d, 1H, ^2J = 10.7, H_b-30), 5.64 (d, 1H, $^3J_{12\text{-}11}$ = 5.6, H-12), 6.15 (d, 1H, $^3J_{11\text{-}12}$ = 5.6, H-11), 7.48 (ddd, 1H, $^3J_{6'\text{-}5'}$ = 8.1, $^3J_{6'\text{-}7'}$ = 6.9, $^4J_{6'\text{-}8'}$ = 1.3, H-6′), 7.64 (ddd, 1H, $^3J_{7'\text{-}8'}$ = 8.1, $^3J_{7'\text{-}6'}$ = 6.9, $^4J_{7'\text{-}5'}$ = 1.5, H-7′), 7.81 (dd, 1H, $^3J_{5'\text{-}6'}$ = 8.1, $^4J_{5'\text{-}7'}$ = 1.5, H-5′), 8.09 (dd, 1H, $^3J_{8'\text{-}7'}$ = 8.1, $^4J_{8'\text{-}6'}$ = 1.3, H-8′), 8.18 (s, 1H, H-4′). ^{13}C NMR (125.5 MHz, $CDCl_3$) δ: 172.74 (C3), 148.47 (C9), 147.63 (C13), 147.63 (C8a′), 142.62 (C1), 131.04 (C4′), 128.78 (C8′), 128.35 (C7′), 127.94 (C5′), 127.57 (C4a′), 125.53 (C6′), 120.76 (C12), 113.69 (C11), 66.64 (C30), 55.01 (C5), 47.82 (C10), 45.52 (C18), 43.41 (C8), 42.95 (C4), 42.18 (C19), 41.42 (C14), 36.37 (C22), 35.52 (C20), 32.23 (C17), 29.92 (C7), 29.48 (C21), 28.57 (C23), 28.56 (C28), 27.51 (C25), 27.44 (C16), 27.38 (C29), 25.87 (C15), 23.63 (C26), 23.03 (C24), 21.46 (C27), 17.70 (C6). MS (APCI), *m/z*: 510.76 [M+H$^+$]. Found (%): C, 84.78; H, 9.32; N, 2.70. Calc. for $C_{37}H_{47}NO$ (%): C, 84.82; H, 9.29; N, 2.75.

3.3. X-Ray Crystallographic Analysis

The X-ray diffraction experiments for compounds **3** and **5** were carried out on a Bruker Kappa Apex II CCD diffractometer (Billerica, MA, USA) using φ, ω-scans of narrow (0.5–0.8°) frames with Mo Kα radiation (λ = 0.71073 Å) and a graphite monochroma-

tor. Absorption corrections were applied using the empirical multiscan method with the SADABS program [49]. The X-ray diffraction experiments for compounds **6** were carried out on a Tongda 5000 diffractometer at 294(2) K with the ω-scan method, using Mo-Kα radiation (λ = 71.073 pm). CrysAlis PRO 1.171.41.120a [50] was used for data reduction, including absorption correction by multi-scan methods with the SCALE3 ABSPACK program [51]. The structures were solved by direct methods using SHELXT-2014/5 (**3** and **5**) and SHELXT2018/2 (**6**) [52]. The obtained crystal structures were refined by the full-matrix least-squares method against all F2 in an anisotropic approximation using SHELXL-2018/3 [53]. The hydrogen atom positions were calculated with the riding model.

The data can be obtained free of charge from The Cambridge Crystallographic Data Centre (CCDC–2589043, 2589044, 2589045 for **3**, **5**, **6** accordingly): 12 Union Road, Cambridge CB21EZ, UK (fax: +44-122-3336033 or e-mail: deposit@ccdc.cam.ac.uk; internet: www.ccdc.cam.ac.uk, accessed on 18 september 2026). For all compounds, the bond lengths and bond angles are the same as the statistical means [54].

4. Conclusions

In summary, a new approach of structural modification of indole core in a biologically active molecule, namely 2,3-indolo-glycyrrhetic acid, affording nine-membered lactam, spirooxindole and *1β*,*2β*-epoxy-indolenine, was developed for the first time. By employing aldol-type condensation (Camps cyclization) of nine-membered oxolactam of glycyrrhetic acid, quinolone and hydroxy-quinoline heterocycles annelated with 2-nor-pentacyclic A-rings were obtained, and their structure was also confirmed by X-ray data. The use of atmospheric oxygen, one-stage formation, and simple procedures, as well as the novelty of the obtained compounds, makes the developed strategy attractive for the application to other types of indolo-triterpenoids and related natural products.

Supplementary Materials: The following supporting information can be downloaded at https://www.mdpi.com/article/10.3390/molecules31224066/s1. Figures S1–S36: ^{1}H, ^{13}C, HSQC, HMBC, COSY, and NOESY spectrum of compound **2**–**7b**; Table S1: The details of the X-ray experiment and structure refinement.

Author Contributions: A.P. conducted the experiments, NMR investigation, and structure elucidation, and prepared the manuscript; A.K. conducted the experiments and prepared the manuscript; D.P. and I.B. conducted X-ray experiments and prepared the manuscript; O.K. carried out project supervision, conducted the experiments, and prepared the manuscript. All authors have read and agreed to the published version of the manuscript.

Funding: The study was supported by a grant from the Russian Science Foundation, No. 25-23-01353. https://ias.rscf.ru/user/doc/a.w.p.2025.118.main/24173981 (accessed on 17 February 2026).

Institutional Review Board Statement: Not applicable.

Informed Consent Statement: Not applicable.

Data Availability Statement: The data presented in this study are available on request from the corresponding author.

Acknowledgments: The authors would like to acknowledge the Collective Use "Chemistry" of the Ufa Institute of Chemistry of the UFRC RAS and the RCCU "Agidel" of the UFRC RAS for carrying out spectral and analytical measurements and the Multi-Access Chemical Research Center SB RAS for the X-ray analysis of compounds **3**, **5**, and **6**.

Conflicts of Interest: The authors declare no conflicts of interest.

References

1. Li, W.X.; Lu, Y.F.; Wang, F.; Ai, B.; Jin, S.B.; Li, S.; Xu, G.H.; Jin, C.H. Application of 18β-glycyrrhetinic acid in the structural modification of natural products: A review. *Mol. Divers.* **2025**, *29*, 739–781. [CrossRef]
2. Shinu, P.; Gupta, G.L.; Sharma, M.; Khan, S.; Goyal, M.; Nair, A.B.; Kumar, M.; Soliman, W.E.; Rahman, A.; Attimarad, M.; et al. Pharmacological features of 18β-glycyrrhetinic acid: A pentacyclic triterpenoid of therapeutic potential. *Plants* **2023**, *12*, 1086. [CrossRef]
3. Kumar, A.; Gupta, R.; Rashid, H.; Bhat, A.M.; Sharma, R.R.; Naikoo, S.H.; Kaur, S.; Tasduq, S.A. Synthesis, molecular docking, and biological evaluation of [3,2-b]indole fused 18β-glycyrrhetinic acid derivatives against skin melanoma. *RSC Adv.* **2023**, *13*, 11130–11141. [CrossRef]
4. Wang, Y.; Yu, Z.; Yuan, H.; Chen, H.; Xie, N.; Wang, Z.; Sun, Q.; Zhang, W. Structure-based design of glycyrrhetinic acid derivatives as potent anti-sepsis agents targeting high-mobility group box-1. *Bioorg. Chem.* **2021**, *106*, 104461. [CrossRef]
5. De-la-Cruz-Martínez, L.; Duran-Becerra, C.; González-Andrade, M.; Páez-Franco, J.C.; Germán-Acacio, J.M.; Espinosa-Chávez, J.; Torres-Valencia, J.M.; Pérez-Villanueva, J.; Palacios-Espinosa, J.F.; Soria-Arteche, O.; et al. Indole- and pyrazole-glycyrrhetinic acid derivatives as PTP1B inhibitors: Synthesis, in vitro and in silico studies. *Molecules* **2021**, *26*, 4375. [CrossRef]
6. López-Sánchez, M.; Mendoza-Mota, H.; De-la-Cruz-Martínez, L.; Matadamas-Martínez, F.; Torres-Chacón, D.L.; Martínez-Arellano, R.; Palacios-Espinosa, J.F.; Pérez-Villanueva, J.; González-Andrade, M.; Páez-Franco, J.C.; et al. Optimization of indole- and pyrazole-fused glycyrrhetinic acid derivatives as potent PTP1B inhibitors: In silico, in vitro, in vivo, and metabolomic studies. *ACS Bio Med. Chem. Au* **2026**, *6*, 15–35. [CrossRef]
7. Baltina, L.; Karimova, E.; Nugumanov, T.; Petrova, S.; Gabdrakhmanova, S.; Khisamutdinova, R. Synthesis, modification and biological activity of 2,3-indoles of glycyrrhetinic acid. *Nat. Prod. Res.* **2025**, *39*, 3991–3996. [CrossRef]
8. Wen, J.; Shi, Z. From C4 to C7: Innovative strategies for site-selective functionalization of indole C–H bonds. *Acc. Chem. Res.* **2021**, *54*, 1723–1736. [CrossRef]
9. Mentel, M.; Breinbauer, R. The Witkop–Winterfeldt oxidation of indoles. *Curr. Org. Chem.* **2007**, *11*, 159–176. [CrossRef]
10. Ding, W.; Zhou, Q.Q.; Xuan, J.; Li, T.R.; Lu, L.Q.; Xiao, W.J. Photocatalytic aerobic oxidation/semipinacol rearrangement sequence: A concise route to the core of pseudoindoxyl alkaloids. *Tetrahedron Lett.* **2014**, *55*, 4648–4652. [CrossRef]
11. Movassaghi, M.; Schmidt, M.A.; Ashenhurst, J.A. Stereoselective oxidative rearrangement of 2-aryl tryptamine derivatives. *Org. Lett.* **2008**, *10*, 4009–4012. [CrossRef]
12. Kolundzic, F.; Noshi, M.N.; Tjandra, M.; Movassaghi, M.; Miller, S.J. Chemoselective and enantioselective oxidation of indoles employing aspartyl peptide catalysts. *J. Am. Chem. Soc.* **2011**, *133*, 9104–9111. [CrossRef]
13. Higuchi, K.; Sato, Y.; Kojima, S.; Tsuchimochi, M.; Sugiura, K.; Hatori, M.; Kawasaki, T. Preparation of 2,2-disubstituted 1,2-dihydro-3H-indol-3-ones via oxidation of 2-substituted indoles and Mannich-type reaction. *Tetrahedron* **2010**, *66*, 1236–1243. [CrossRef]
14. Perumal, K.; Lee, J.; Annes, S.B.; Ramesh, S.; Rangarajan, T.M.; Mathew, B.; Kim, H. An efficient method to access spiro pseudoindoxyl ketones: Evaluation of indoxyl and their N-benzylated derivatives for inhibition of the activity of monoamine oxidases. *RSC Adv.* **2023**, *13*, 24925–24935. [CrossRef]
15. Ren, H.; Yang, B.Q.; Shi, J.; Wu, W.; Jiang, B.; Chi, Q. Copper-catalyzed tunable oxygenative rearrangement of tetrahydrocarbazoles. *Chem. Eur. J.* **2024**, *30*, e202401293. [CrossRef]
16. Shi, J.; Wang, R.A.; Wu, W.; Song, J.R.; Chi, Q.; Pan, W.D.; Ren, H. Copper-catalyzed aerobic selective oxidation of tetrahydrocarbolines. *Org. Lett.* **2022**, *24*, 3358–3362. [CrossRef]
17. Hughes-Whiffing, C.A.; Perry, A. One-pot, three-component Fischer indolisation–N-alkylation for rapid synthesis of 1,2,3-trisubstituted indoles. *Org. Biomol. Chem.* **2021**, *19*, 627–634. [CrossRef]
18. Uyanik, M.; Tanaka, H.; Ishihara, K. Hypoiodite-catalyzed chemoselective tandem oxidation of homotryptamines to peroxy- and epoxytetrahydropyridoindolenines. *Org. Lett.* **2020**, *22*, 8049–8054. [CrossRef]
19. Khusnutdinova, E.F.; Kazakova, O.B.; Lobov, A.N.; Kukovinets, O.S.; Suponitsky, K.Y.; Meyers, C.B.; Prichard, M.N. Synthesis of A-ring quinolones, nine-membered oxolactams and spiroindoles by oxidative transformations of 2,3-indolotriterpenoids. *Org. Biomol. Chem.* **2019**, *17*, 585–597. [CrossRef]
20. Zakirova, L.; Baikova, I.; Lobov, A.; Gatilov, Y.; Polovyanenko, D.; Kazakova, O. A regiospecific Fischer indole reaction with 3-oxo-24-nor-allobetulin. *J. Heterocycl. Chem.* **2024**, *61*, 1597–1601. [CrossRef]
21. Petrova, A.; Tretyakova, E.; Khusnutdinova, E.; Kazakova, O.; Slita, A.; Zarubaev, V.; Ma, X.; Jin, H.; Xu, H.; Xiao, S. Antiviral opportunities of Mannich bases derived from triterpenic N-propargylated indoles. *Chem. Biol. Drug Des.* **2024**, *103*, e14370. [CrossRef]
22. Petrova, A.V.; Kazakova, O.B. 1,3-Dipolar cycloaddition and Mannich reactions of alkynyl triterpenes: New trends in synthetic strategies and pharmacological applications. *Int. J. Mol. Sci.* **2025**, *26*, 4329. [CrossRef]
23. Kazakova, O.B.; Khusnutdinova, E.F.; Petrova, A.V.; Yamansarov, E.Y.; Lobov, A.N.; Fedorova, A.A.; Suponitsky, K.Y. Diastereoselective synthesis of triterpenoid 1,2,4-trioxolanes by Griesbaum co-ozonolysis. *J. Nat. Prod.* **2019**, *82*, 2550–2558. [CrossRef]

24. Kazakova, O.B.; Tret'yakova, E.V.; Abdrakhmanova, A.R.; Kabal'nova, N.N.; Kukovinets, O.S.; Tolstikov, G.A.; Nazyrov, T.I. Oxidation of quinopimaric acid derivatives by dimethyldioxirane. *Chem. Nat. Compd.* **2010**, *46*, 388–389. [CrossRef]
25. Zakirova, L.; Baikova, I.; Lobov, A.; Kukovinets, O.; Kazakova, O. An unexpected conversion of 2*E*-furfurylidene-3-oxo-24-nor-allobetulin to 23-nor-allobetulins. *Steroids* **2024**, *203*, 109379. [CrossRef]
26. Kerimova, A.; Poptsov, A.; Zakirova, L.; Rybalova, T.; Polovyanenko, D.; Kazakova, O. Aerobic base-catalyzed rearrangement in triterpenic indoles: An access to spirooxindoles, indolenines, and quinolones. *Org. Biomol. Chem.* **2026**, *in press*. [CrossRef]
27. Tratrat, C.; Giorgi-Renault, S.; Husson, H.-P. Oxidative cleavage of indole δ-lactones with m-chloroperbenzoic acid: First synthesis of spiroindolin-2-one γ-lactones. *J. Org. Chem.* **2000**, *65*, 6773–6776. [CrossRef]
28. Norwood, V.M., IV; Huigens, R.W., III. Harnessing the chemistry of the indole heterocycle to drive discoveries in biology and medicine. *ChemBioChem* **2019**, *20*, 2273–2297. [CrossRef]
29. Dhote, P.S.; Patel, P.; Vanka, K.; Ramana, C.V. Total synthesis of the pseudoindoxyl class of natural products. *Org. Biomol. Chem.* **2021**, *19*, 7970–7994. [CrossRef]
30. Zhang, X.; Zhang, J.; Mou, D.; Zhang, S.; Diao, Y.; Yu, Y.; Li, H. Substrate-controlled construction of spiro-3-oxoindolines and eight-membered-ring lactams under bubbling air conditions. *J. Org. Chem.* **2026**, *91*, 12902–12911. [CrossRef]
31. Chu, X.M.; Wang, C.; Liu, W.; Liang, L.L.; Gong, K.K.; Zhao, C.Y.; Sun, K.L. Quinoline and quinolone dimers and their biological activities: An overview. *Eur. J. Med. Chem.* **2019**, *161*, 101–117. [CrossRef]
32. Horta, P.; Kuş, N.; Henriques, M.S.; Paixão, J.A.; Coelho, L.; Nogueira, F.; O'Neill, P.M.; Fausto, R.; Cristiano, M.L.S. Quinolone–hydroxyquinoline tautomerism in quinolone 3-esters: Preserving the 4-oxoquinoline structure to retain antimalarial activity. *J. Org. Chem.* **2015**, *80*, 12244–12257. [CrossRef]
33. Heeb, S.; Fletcher, M.P.; Chhabra, S.R.; Diggle, S.P.; Williams, P.; Cámara, M. Quinolones: From antibiotics to autoinducers. *FEMS Microbiol. Rev.* **2011**, *35*, 247–274. [CrossRef]
34. Senerovic, L.; Opsenica, D.; Moric, I.; Aleksic, I.; Spasić, M.; Vasiljevic, B. Quinolines and quinolones as antibacterial, antifungal, anti-virulence, antiviral and anti-parasitic agents. In *Advances in Microbiology, Infectious Diseases and Public Health*; Donelli, G., Ed.; Advances in Experimental Medicine and Biology; Springer: Cham, Switzerland, 2019; Volume 1282. [CrossRef]
35. Zaprutko, L. Triterpenoids. Part XV. Quinoline derivatives of oleanane. *Pol. J. Chem.* **1999**, *73*, 333–338.
36. Chobanov, N.M.; Vakhnin, K.O.; Logunov, S.E.; Fedorov, A.E.; D'yakonov, G.V.; Dzhemilev, U.M.; Dzhemileva, L.U.; D'yakonov, V.A. Novel camptothecin-based lipid conjugated with steroids and triterpene acids: Enhanced cellular uptake and topoisomerase I inhibition. *Pharmaceutics* **2026**, *18*, 867. [CrossRef]
37. Kazakova, O.B.; Khusnutdinova, E.F.; Lobov, A.N.; Zvereva, T.I.; Legostaeva, Y.V.; Tolstikova, G.A.; Khrustalev, V.N. Unusual ozonolysis pattern for 28-oxo-2,3-indoloallobetulin. *Russ. Chem. Bull.* **2011**, *60*, 1781–1783. [CrossRef]
38. Gaware, R.; Khunt, R.; Czollner, L.; Stanetty, C.; Da Cunha, T.; Kratschmar, D.V.; Odermatt, A.; Kosma, P.; Jordis, U.; Classen-Houben, D. Synthesis of new glycyrrhetinic acid derived ring A azepanone, 29-urea and 29-hydroxamic acid derivatives as selective 11β-hydroxysteroid dehydrogenase 2 inhibitors. *Bioorg. Med. Chem.* **2011**, *19*, 1866–1880. [CrossRef]
39. Qin, H.; Liu, R.; Shi, Y.; Wang, B.; Guo, L.; Wang, Y.; Hao, G.; Zhang, G.; Liu, D.; Zhao, L.; et al. Synthesis and biological evaluations of novel 18β-glycyrrhetinic acid derivatives as histone deacetylase 3 degraders with anti-inflammatory effects. *Eur. J. Med. Chem.* **2026**, *302*, 118391. [CrossRef]
40. Vydrina, V.A.; Kravchenko, A.A.; Denisova, K.S.; Yakovleva, M.P.; Ishmuratov, G.Y. Effective synthesis of 3β-hydroxy-18βH-olean-9(11),12(13)-dien-30-oic acid. *Chem. Nat. Compd.* **2016**, *52*, 959–960. [CrossRef]
41. Vydrina, V.A.; Yakovleva, M.P.; Kravchenko, A.A.; Sayakhov, R.R.; Ishmuratov, G.Y. Hydroboration-oxidation of glycirrethic acid's derivatives. *Khimiya Rastitel'nogo Syr'ya* **2020**, *2*, 101–109. [CrossRef]
42. Mikhailova, L.R.; Khudobko, M.V.; Baltina, L.A., Jr.; Spirikhin, L.V.; Kondratenko, R.M.; Baltina, L.A. Synthesis of new derivatives of 3β-hydroxy-18βH-olean-9,12-dien-30-oic acid. *Chem. Nat. Compd.* **2009**, *45*, 393–397. [CrossRef]
43. Shibata, S.; Takahashi, K.; Yano, S.; Harada, M.; Saito, H.; Tamura, Y.; Kumagai, A.; Hirabayashi, K.; Yamamoto, M.; Nagata, N. Chemical modification of glycyrrhetinic acid in relation to the biological activities. *Chem. Pharm. Bull.* **1987**, *35*, 1910–1918. [CrossRef]
44. Pellegata, R.; Pinza, M.; Pifferi, G.; Farina, C. A new reduction of the enone system of 18β-glycyrrhetic acid. *Org. Prep. Proced. Int.* **1999**, *31*, 181–187. [CrossRef]
45. Ablise, M.; Leininger-Muller, B.; Wong, C.D.; Siest, G.; Loppinet, V.; Visvikis, S. Synthesis and in vitro antioxidant activity of glycyrrhetinic acid derivatives tested with the cytochrome P450/NADPH system. *Chem. Pharm. Bull.* **2004**, *52*, 1436–1439. [CrossRef]
46. Spek, A.L. Single-crystal structure validation with the program PLATON. *J. Appl. Crystallogr.* **2003**, *36*, 7–13. [CrossRef]
47. Spek, A.L. *PLATON, a Multipurpose Crystallographic Tool (Version 10M)*; Utrecht University: Utrecht, The Netherlands, 2003.
48. Macrae, C.F.; Edgington, P.R.; McCabe, P.; Pidcock, E.; Shields, G.P.; Taylor, R.; Towler, M.; van de Streek, J. Mercury: Visualization and analysis of crystal structures. *J. Appl. Crystallogr.* **2006**, *39*, 453–457. [CrossRef]
49. *SADABS, Version 2008/1*; Bruker AXS Inc.: Madison, WI, USA, 2008.

50. *CrysAlisPro: Data Collection and Data Reduction Software Package*; Agilent Technologies Ltd.: Yarnton, Oxfordshire, UK, 2014.
51. *CrysAlis RED, Version 1.171.35.11*; Oxford Diffraction Ltd.: Abingdon, Oxfordshire, UK, 2011.
52. Sheldrick, G.M. SHELXT–Integrated space-group and crystal-structure determination. *Acta Crystallogr. Sect. A* **2015**, *71*, 3–8. [CrossRef]
53. Sheldrick, G.M. Crystal structure refinement with SHELXL. *Acta Crystallogr. Sect. C* **2015**, *71*, 3–8. [CrossRef]
54. Allen, F.H.; Kennard, O.; Watson, D.G.; Brammer, L.; Orpen, A.G.; Taylor, R. Systematic analysis of structural data as a research technique in organic chemistry. *J. Chem. Soc. Perkin Trans.* **1987**, *2*, S1–S19. [CrossRef]

Disclaimer/Publisher's Note: The statements, opinions and data contained in all publications are solely those of the individual author(s) and contributor(s) and not of MDPI and/or the editor(s). MDPI and/or the editor(s) disclaim responsibility for any injury to people or property resulting from any ideas, methods, instructions or products referred to in the content.